The Nonuniform Discrete Fourier Transform and Its Applications in Filter Design: Part I—1-D

Sonali Bagchi, *Member, IEEE*, and Sanjit K. Mitra, *Fellow, IEEE*

***Abstract*—The *nonuniform discrete Fourier transform* (NDFT) of a sequence of length N is defined as samples of its z-transform evaluated at N distinct points located arbitrarily on the z-plane. The NDFT reduces to the conventional discrete Fourier transform (DFT) when these points are located on the unit circle at equally spaced angles. The flexibility offered by the NDFT in choosing the sampling points leads to a variable spectral resolution that can be controlled by the user. The NDFT is applied to nonuniform frequency sampling design of 1-D FIR filters. This method produces nearly optimal equiripple 1-D filters with greatly reduced design times as compared with the Parks–McClellan algorithm. Comparisons with filters designed by other methods are presented to demonstrate the effectiveness of the proposed method.**

I. Introduction

THE DISCRETE Fourier transform (DFT) is an important tool in signal processing applications. Given a sequence $x[n]$ of length N, the DFT evaluates its z-transform $X(z)$ at N equally spaced angles on the unit circle in the z-plane. The DFT is widely used because it can be computed efficiently by fast Fourier transform (FFT) algorithms. However, the DFT gives only equally spaced samples on the unit circle. This implies that it has a fixed spectral resolution which depends only on the number of points. In an attempt to obtain a more general sampling of the z-transform, Rabiner *et al.* [1] introduced the chirp z-transform (CZT). This algorithm computes samples of the z-transform at M points which lie on circular or spiral contours in the z-plane beginning at any arbitrary point. The angular spacing of these points is constant. For example, if we want to compute samples of $X(z)$ that are equally spaced within a particular region of the unit circle, the CZT can be used. To obtain unequally spaced samples on the unit circle, Oppenheim and Johnson introduced a technique for computing spectra with unequal resolution using the FFT [2]. In this method, the original sequence $x[n]$ is transformed to a new sequence having the property that its DFT is equal to samples of $X(z)$ at unequally spaced angles around the unit circle. An allpass network is used to implement a distortion of the frequency axis. Therefore, the new sequence is of infinite length and a finite-length window must be applied to it before its FFT can be computed. Since this causes a smearing of the spectrum before the spectral samples can be taken, the method gives only approximate results.

The idea of nonuniform frequency sampling has been used in various applications such as spectral analysis [2] and filter design [3]–[5]. In this paper, we develop a basic framework for nonuniform sampling by generalizing the definition of the DFT. The *nonuniform discrete Fourier transform* (NDFT) of a sequence of length N is defined as a sequence of samples of its z-transform evaluated at N distinct points located arbitrarily on the z-plane [6]. The conventional DFT is a special case of the NDFT, obtained when the sampling points are located on the unit circle at equally spaced angles. The flexibility offered by the NDFT in choosing the points on the z-plane can be utilized in many signal processing applications. Here, we develop the application of the NDFT in one-dimensional (1-D) finite-impulse-response (FIR) filter design. In a companion paper [7], the concept of the NDFT is extended to two dimensions and is applied to the design of two-dimensional (2-D) FIR filters.

This paper is organized as follows. The NDFT is introduced in Section II. In Section III, we propose a nonuniform frequency sampling technique for designing 1-D FIR filters. This NDFT-based method is then developed for designing various types of filters. Design examples are presented to demonstrate the effectiveness of the proposed method, as compared with existing methods such as uniform frequency sampling and the Parks–McClellan algorithm. Section IV provides the concluding remarks.

Manuscript received August December 1, 1994; revised September 5, 1995. This work was supported by University of California MICRO Grants, with matching funds from Tektronix, Inc., Rockwell International Corp., and Digital Instruments, Inc. This paper was recommended by Associate Editor P. A. Regalia.

S. Bagchi was with the Department of Electrical and Computer Engineering, University of California, Santa Barbara, CA 93106 USA. She is now with AT&T Bell Laboratories, Allentown, PA 18103 USA.

S. K. Mitra is with the Department of Electrical and Computer Engineering, University of California, Santa Barbara, CA 93106 USA.

Publisher Item Identifier S 1057-7130(96)03759-7.

II. Definition and Properties

The *nonuniform discrete Fourier transform* (NDFT) of a sequence $x[n]$ of length N is defined as

$$X(z_k) = \sum_{n=0}^{N-1} x[n] z_k^{-n}, \quad k = 0, 1, \cdots, N-1 \qquad (1)$$

where $z_0, z_1, \cdots, z_{N-1}$ are distinct points located arbitrarily on the z-plane. We can express (1) in a matrix form as

$$\mathbf{X} = \mathbf{D}\mathbf{x} \tag{2}$$

where

$$\mathbf{X} = \begin{bmatrix} X(z_0) \\ X(z_1) \\ \vdots \\ X(z_{N-1}) \end{bmatrix}$$

$$\mathbf{x} = \begin{bmatrix} x[0] \\ x[1] \\ \vdots \\ x[N-1] \end{bmatrix} \tag{3}$$

and

$$\mathbf{D} = \begin{bmatrix} 1 & z_0^{-1} & z_0^{-2} & \cdots & z_0^{-(N-1)} \\ 1 & z_1^{-1} & z_1^{-2} & \cdots & z_1^{-(N-1)} \\ \vdots & \vdots & \vdots & \ddots & \vdots \\ 1 & z_{N-1}^{-1} & z_{N-1}^{-2} & \cdots & z_{N-1}^{-(N-1)} \end{bmatrix}. \tag{4}$$

Note that the NDFT matrix $\mathbf{D}$ is a Vandermonde matrix, fully specified by the choice of the N points z_k. It can be shown [8] that the determinant of $\mathbf{D}$ can be expressed in a factored form as

$$\det(\mathbf{D}) = \prod_{i \neq j, i > j} (z_i^{-1} - z_j^{-1}). \tag{5}$$

Consequently, $\mathbf{D}$ is nonsingular provided the N sampling points $z_0, z_1, \cdots, z_{N-1}$ are distinct. Thus, the inverse NDFT exists and is unique, as given by

$$\mathbf{x} = \mathbf{D}^{-1}\mathbf{X}. \tag{6}$$

The problem of computing the inverse NDFT $\mathbf{x}$ is equivalent to solving the Vandermonde system in (2), which involves $O(N^3)$ operations. This can be alternatively stated as a polynomial interpolation problem, which arises in many areas of engineering and numerical analysis. Therefore, existing methods such as Lagrange and Newton interpolation can also be used. The latter involves $O(N^2)$ operations, and thus provides a more efficient method of solving for the inverse NDFT. Unlike the DFT, there is no implicit periodicity in the general NDFT representation of finite-length sequences. Consequently, algorithms as fast as the FFT cannot be developed for computing the inverse NDFT. However, this does not cause problems in practical applications which benefit from the flexibility in sampling provided by the NDFT.

The properties of the NDFT are analogous to those of the z-transform and Fourier transform. These include linearity, shifting in the time domain, scaling and shifting in the z-domain, time reversal, and symmetry properties, details of which are provided in [9]. Due to the lack of periodicity in the general NDFT representation, some properties of the DFT such as circular shift and duality do not hold for the NDFT. Linear convolution of two sequences can be computed using the NDFT [9]. The sequences are zero-padded, their NDFT's are multiplied, and an inverse NDFT is then applied to the result. This is similar to the process of computing linear convolution using the DFT [10].

III. 1-D FIR Filter Design Using the NDFT

We propose an FIR filter design method based on nonuniform frequency sampling. The resulting filters are nearly equal to optimal (minimax) filters designed with the same specifications. Additionally, the filter design times are much lower than those required by the Parks–McClellan algorithm [11] for optimal filter design.

In the traditional frequency sampling approach to FIR filter design, the desired frequency response is sampled at N *equally spaced* frequencies, where N is the filter length. Since the frequency samples are simply the DFT coefficients of the filter impulse response, an N-point inverse DFT is used to compute the filter coefficients. The interpolated frequency response has considerable ripple in regions where there are sudden transitions in the desired response, e.g., near the bandedges of band-selective filters. To improve the filter characteristics, a transition band has been introduced in the desired frequency response. In one such method [3], a number of samples in the transition band are varied in amplitude so as to minimize the maximum deviation from the desired response over some frequency range of interest. Linear programming is used to optimize the values of these variable samples. Besides being computationally intensive, this method does not provide good control over typical filter specifications such as bandedges and peak ripple. An improved uniform frequency sampling technique [12] uses a desired response that is a simple analytic function with a few degrees of freedom. The parameters controlling the desired response are chosen in such a way that the response can be realized almost exactly by an FIR filter. This analytic function is sampled uniformly to obtain frequency samples, whose inverse DFT then gives the filter coefficients.

A brief discussion of the technique of *nonuniform frequency sampling* was included in [3]. However, the authors considered low-pass filter design examples using only two sets of nonuniform data. The results obtained were not entirely encouraging and led them to stress that more work would have to be done to fully utilize the advantages of nonuniform frequency sampling. Note that we can apply the Lagrange interpolation formula [3] to express the z-transform of the filter $H(z)$ in the form

$$H(z) = \sum_{k=0}^{N-1} \frac{H_k \sum_{i=0}^{N-1} b_i z^{-i}}{\alpha_k (1 - z_k z^{-1})} \tag{7}$$

where

$$H_k = H(z_k), \quad k = 0, 1, \cdots, N-1,$$
$$\alpha_k = \prod_{i \neq k} (1 - z_i z_k^{-1})$$

and the coefficients b_i satisfy

$$\sum_{i=0}^{N-1} b_i z^{-i} = \prod_{i=0}^{N-1} (1 - z_i z^{-1}).$$

Although $H(z)$ is a linear function of the sample values H_k, it is a nonlinear function of the sample locations z_k. Thus, we have to resort to complex nonlinear optimization techniques if we want to choose the values as well as the locations of the frequency samples, so as to minimize the peak ripple of the frequency response in some band. In a recent effort on nonuniform frequency sampling [4], a Newton-type polynomial with complex conjugate coefficients is used for interpolating the desired complex frequency response of a real-coefficient FIR filter. In another paper [5], zero-phase FIR filters are designed by introducing a class of Newton polynomials that satisfies the symmetry properties imposed by such filters.

A. Proposed Nonuniform Frequency Sampling Design

In the proposed FIR filter design method, the desired frequency response is sampled at N nonuniformly spaced points on the unit circle in the z-plane. An N-point inverse NDFT of these frequency samples gives the filter coefficients. We address the problem of nonuniform frequency sampling design by considering the two major issues involved: 1) the generation of the desired frequency response for the given filter specifications, and 2) the choice of the frequency-sample locations. The aim is to obtain a filter whose interpolated frequency response is nearly equiripple in each band. The approaches used for these two issues are outlined here.

1) Generation of the Desired Frequency Response: Given the filter specifications, we construct the desired frequency response by using a separate *analytic function* for each frequency band. The equiripple nature of the response is obtained by using Chebyshev polynomials and a suitable transformation to map the domain of the polynomial to the frequency axis. Each function involves several parameters which are found by imposing appropriate constraints so as to obtain the desired mapping.

2) Choice of the Frequency-Sample Locations: In addressing this issue, we must note that there is no good analytic approximation for the frequency response in the transition band. We have found that the best locations for the frequency samples are the *extrema* of the desired equiripple response (see Section III-H). As the desired response is approximated by analytic functions, the extremal frequencies can be expressed in closed form. In addition, since the total number of extrema is related to the filter length, we do not need to place any extra samples in the transition band. However, in special cases (e.g., for designing filters with very wide transition bands), we can place a few transition samples to constrain any possible overshoot within this band.

Once we have addressed these issues, we can refer to the NDFT formulation in (1). The NDFT matrix $\mathbf{D}$ is constructed from the frequency-sample locations found in Step 2. Samples of the analytic functions generated in Step 1 are used to construct the NDFT vector $\mathbf{X}$. The filter impulse response $\mathbf{x}$ is then obtained by solving this linear system of equations. Note that all known symmetries in the filter impulse response can be utilized to reduce the number of independent filter coefficients. This results in a smaller linear system and, therefore, reduced design time.

We can use the proposed method to design various types of linear-phase FIR filters (of length N), such as low-pass filters (Type I if N is odd, Type II if N is even), high-pass filters (Type I if N is odd, Type IV if N is even), band-pass filters (Types I or III if N is odd, Types II or IV if N is even), and Mth-band filters such as third-band filters (Type I). We now describe the design method in detail by considering a few of these filters.

B. Low-Pass Filter Design (Type I)

Let us consider the design of a linear-phase low-pass filter of Type I. The filter has a symmetric impulse response

$$h[n] = h[N-1-n], \quad n = 0, 1, \cdots, N-1 \tag{8}$$

where the filter length N is an odd integer. The frequency response of the filter is

$$H(\omega) = \sum_{n=0}^{N-1} h[n] e^{-j\omega n}. \tag{9}$$

By applying the symmetry condition in (8), this can be expressed in the form [10]

$$H(\omega) = A(\omega) e^{-j\omega(N-1)/2} \tag{10}$$

where $A(\omega)$ is a real, even, periodic function of ω, given by

$$A(\omega) = \sum_{k=0}^{(N-1)/2} a[k] \cos \omega k \tag{11}$$

and

$$\begin{aligned} a[0] &= h\left[\frac{N-1}{2}\right], \\ a[k] &= 2h\left[\frac{N-1}{2} - k\right], \quad k = 1, 2, \cdots, \frac{N-1}{2}. \end{aligned} \tag{12}$$

Let the filter have its passband edge at ω_p, stopband edge at ω_s, and peak ripples δ_p and δ_s in the passband and stopband, respectively. We proceed with the design by considering the two issues involved:

1) Generation of the Desired Frequency Response: The real-valued amplitude response $A(\omega)$ is represented by analytic functions [12] as follows:

$$A(\omega) = \begin{cases} H_p(\omega) = 1 - \delta_p T_P[X_p(\omega)], & 0 \le \omega \le \omega_p, \\ H_s(\omega) = \delta_s T_S[X_s(\omega)] & \omega_s \le \omega \le \pi. \end{cases} \tag{13}$$

Here, $T_M(\cdot)$ denotes a Chebyshev polynomial of order M, defined as

$$T_M(x) = \begin{cases} \cos[M \cos^{-1}(x)], & -1 \le x \le 1, \\ \cosh[M \cosh^{-1}(x)], & \text{otherwise.} \end{cases} \tag{14}$$

Note that $T_M(x)$ is equiripple in the range $-1 \le x \le 1$ and monotone outside this range. Depending on whether M is even or odd, $T_M(x)$ is an even or odd function of x, respectively. The integers P and S are given by

$$P = N_p, \tag{15}$$

$$S = N_s \tag{16}$$

where N_p equals the number of extrema in the passband $0 \leq \omega \leq \omega_p$, and N_s equals the number of extrema in the stopband $\omega_s \leq \omega \leq \pi$. The functions $X_p(\omega)$ and $X_s(\omega)$ are required to map the equiripple interval $-1 \leq x \leq 1$ of $T_P(x)$ and $T_S(x)$ to the passband and stopband, respectively. This mapping is obtained by using the transformations

$$X_p(\omega) = A \cos(a\omega + b) + B, \tag{17}$$

$$X_s(\omega) = C \cos(c\omega + d) + D. \tag{18}$$

The values for the eight parameters A, B, C, D, a, b, c, and d, are obtained by imposing appropriate constraints on the functions, $H_p(\omega)$ and $H_s(\omega)$ [9], [12]

$$H_p(\omega) = H_p(-\omega) \tag{19}$$

$$H_s(\pi + \omega) = H_s(\pi - \omega) \tag{20}$$

$$H_p(\omega_p) = 1 - \delta_p \tag{21}$$

$$H_s(\omega_s) = \delta_s, \tag{22}$$

$$H_p(0) = \begin{cases} 1 + \delta_p, & P = \text{odd} \\ 1 - \delta_p, & P = \text{even} \end{cases} \tag{23}$$

$$H_s(\pi) = \begin{cases} -\delta_s, & S = \text{odd} \\ \delta_s, & S = \text{even}, \end{cases} \tag{24}$$

$$\min[H_p(\omega)] = -\delta_s \tag{25}$$

$$\max[H_s(\omega)] = 1 + \delta_p. \tag{26}$$

These lead to the following expressions for the parameters

$$A = \frac{1}{2}\left\{T_P^{-1}\left(\frac{1+\delta_s}{\delta_p}\right) + 1\right\} \tag{27}$$

$$B = A - 1 \tag{28}$$

$$C = \frac{1}{2}\left\{T_S^{-1}\left(\frac{1+\delta_p}{\delta_s}\right) + 1\right\} \tag{29}$$

$$D = C - 1 \tag{30}$$

$$a = \frac{1}{\omega_p}\cos^{-1}\left(\frac{B-1}{A}\right) \tag{31}$$

$$b = \pi, \tag{32}$$

$$c = \frac{1}{\omega_s - \pi}\cos^{-1}\left(\frac{D-1}{C}\right) \tag{33}$$

$$d = \pi(1 - c). \tag{34}$$

Given the filter specifications, N, ω_p, ω_s and $k = \delta_p/\delta_s$, we estimate the ripple sizes δ_p and δ_s from [10]

$$N = \frac{-10\log_{10}(\delta_p\delta_s) - 13}{2.324(\omega_s - \omega_p)} + 1 \tag{35}$$

which gives

$$\delta_p = \sqrt{k}\, 10^{-0.1162(\omega_s - \omega_p)(N-1) - 0.65} \tag{36}$$

and

$$\delta_s = \frac{\delta_p}{k}. \tag{37}$$

Alternatively, if we are given ω_p, ω_s, δ_p, and δ_s, we can estimate the required filter length N from (35). The Chebyshev polynomial orders P and S are then determined. Since they correspond to the number of extrema in the passband and stopband respectively, they are found by weighting them in proportion to the sizes of the passband and stopband such that $P + S = (N-1)/2$. Note that $P + S$ equals the total number of alternations in the filter response over the range $0 \leq \omega \leq \pi$, excluding those at the bandedges, ω_p and ω_s. The alternation theorem states that an optimum Type I filter must have a minimum of $(L+2)$ alternations, where $L = (N-1)/2$. Thus, we obtain

$$P + S = L = \frac{N-1}{2}. \tag{38}$$

2) Choice of the Frequency-Sample Locations: Since the impulse response of the filter is symmetric, as shown in (8) the number of independent coefficients in a Type I filter is given by

$$N_i = \frac{N+1}{2}. \tag{39}$$

Thus, we need only N_i samples located in the range $0 \leq \omega \leq \pi$. These samples are placed at the extrema of the desired response which has been approximated by analytic functions in Step 1.

The P extrema of $H_p(\omega)$ occur when

$$H_p(\omega) = 1 \pm \delta_p \tag{40}$$

or

$$X_p(\omega) = \cos\left(\frac{k\pi}{P}\right), \quad k = 1, 2, \cdots, P. \tag{41}$$

Using the definition for $X_p(\omega)$ in (17), we obtain the extrema in the passband

$$\omega_k^{(p)} = \frac{1}{a}\left\{\cos^{-1}\left[\frac{\cos\left(\frac{k\pi}{P}\right) - B}{A}\right] - b\right\}$$
$$k = 1, 2, \cdots, N_p. \tag{42}$$

Similarly, the S extrema of $H_s(\omega)$ occur when

$$H_s(\omega) = \pm\delta_s. \tag{43}$$

This leads to the following expression for the extrema in the stopband

$$\omega_k^{(s)} = \frac{1}{c}\left\{\cos^{-1}\left[\frac{\cos\left(\frac{k\pi}{S}\right) - D}{C}\right] - d\right\}$$
$$k = 1, 2, \cdots, N_s. \tag{44}$$

From (38) and (39), we observe that $P + S = N_i - 1$. Therefore, we need one more sample besides those at the $P+S$ extrema. This sample is placed either at the passband edge ω_p, or at the stopband edge ω_s.

Thus, we sample the functions generated in Step 1 at the locations obtained in Step 2, and then solve for the N_i independent filter coefficients. We can also design *high-pass* filters directly using the proposed method with minor modifications, by mapping the function $H_s(\omega)$ to the low-frequency band and $H_p(\omega)$ to the high-frequency band. Of course, high-pass

filter design can also be achieved by designing an appropriate low-pass filter $h[n]$ and transforming it to a high-pass filter, whose coefficients are then given by $(-1)^n h[n]$.

Half-band FIR filters belong to a special class of Type I FIR filters. The design procedure is further simplified because every other sample in the half-band impulse response is zero. The number of independent filter coefficients is given by

$$N_i = \left\lceil \frac{N-1}{4} \right\rceil. \tag{45}$$

Due to the symmetry in the frequency response of the filter

$$H(\omega) + H(\pi - \omega) = 1 \tag{46}$$

the orders of the Chebyshev polynomials approximating the passband and stopband are equal

$$\begin{aligned} P &= S \\ &= N_i. \end{aligned} \tag{47}$$

The symmetry between the passband and stopband also results in fewer parameters controlling the functions $H_p(\omega)$ and $H_s(\omega)$. We need to generate only the four parameters, A, B, a, and b. Then, we obtain N_i samples at the P extrema of the passband function $H_p(\omega)$, as given in (42). This illustrates the flexibility of our design method, as compared with uniform frequency sampling. Besides, the design time is reduced nearly by *half*, as compared with that required by a general symmetric FIR filter of the same length.

C. Low-Pass Filter Design (Type II)

We shall now modify the method discussed in Section III-B, so as to design a linear-phase low-pass filter of Type II. Such a filter has a symmetric impulse response as shown in (8), where the filter length N is an even integer. The frequency response of the filter can be expressed as [10]

$$H(\omega) = B(\omega) e^{-j\omega(N-1)/2} \tag{48}$$

where $B(\omega)$ is a real, even, periodic function of ω, given by

$$B(\omega) = \sum_{k=1}^{N/2} b[k] \cos\left[\omega\left(k - \tfrac{1}{2}\right)\right] \tag{49}$$

and

$$b[k] = 2h\left[\frac{N}{2} - k\right], \quad k = 1, 2, \cdots, \frac{N}{2}. \tag{50}$$

The real-valued amplitude response $B(\omega)$ is represented by

$$B(\omega) = \begin{cases} H_p(\omega) = 1 - \delta_p T_P[X_p(\omega)], & 0 \le \omega \le \omega_p, \\ H_s(\omega) = \delta_s T_S[X_s(\omega)], & \omega_s \le \omega \le \pi. \end{cases} \tag{51}$$

In this case, the orders of the Chebyshev polynomials in the passband and stopband are given by

$$P = N_p \tag{52}$$

$$S = 2N_s + 1 \tag{53}$$

where N_p and N_s equal the number of extrema in the passband and stopband regions, respectively. Equation (53) arises because the Type II response $B(\omega)$ has a zero at $\omega = \pi$, and is antisymmetric about this point in frequency. Therefore, the Chebyshev polynomial $T_S(x)$ must be antisymmetric, i.e., its order S must be odd, as shown in (53). The equiripple interval $0 \le x \le 1$ of $T_S(x)$ is mapped by the function $X_s(\omega)$ to the stopband $\omega_s \le \omega \le \pi$. As discussed in Section III-B, the equiripple interval $-1 \le x \le 1$ of $T_P(x)$ is mapped to the passband $0 \le \omega \le \omega_p$ by the function $X_p(\omega)$. This mapping is obtained by choosing the functions $X_p(\omega)$ and $X_s(\omega)$ of the form shown in (17) and (18).

To obtain closed-form expressions for the eight parameters, A, B, C, D, a, b, c, and d, we impose appropriate constraints on the functions, $H_p(\omega)$ and $H_s(\omega)$, as shown in Section III-B. The only modifications required for Type II filters arise because the response $B(\omega)$ is antisymmetric about the point $\omega = \pi$, and $B(\pi) = 0$. Thus, we have the new constraints

$$H_s(\pi + \omega) = -H_s(\pi - \omega) \tag{54}$$

$$H_s(\pi) = 0 \tag{55}$$

instead of those in (20) and (24). As derived in [9], these lead to new expressions for the following parameters:

$$C = T_S^{-1}\left(\frac{1+\delta_p}{\delta_s}\right), \tag{56}$$

$$D = 0, \tag{57}$$

$$c = \frac{1}{\pi - \omega_s} \sin^{-1}\left(\frac{1}{C}\right) \tag{58}$$

$$d = \frac{\pi}{2}(1 - 2c). \tag{59}$$

In the Type II case, the Chebyshev polynomial orders P and S are determined from (52) and (53). N_p and N_s are first found by weighting them in proportion to the sizes of the passband and stopband such that $N_p + N_s = (N/2) - 1$. Note that $N_p + N_s$ equals the total number of alternations in the frequency response over the range $0 \le \omega \le \pi$, excluding those at the bandedges, ω_p and ω_s. The alternation theorem states [10] that an optimum Type II filter must have a minimum of $(L+2)$ alternations, where $L = (N/2) - 1$. Thus, we have

$$\begin{aligned} N_p + N_s &= L \\ &= \frac{N}{2} - 1. \end{aligned} \tag{60}$$

Due to the symmetry in the impulse response, the number of independent coefficients in a Type II filter is given by

$$N_i = \frac{N}{2}. \tag{61}$$

Thus, we place N_i samples at the extrema of the desired response in the frequency range $0 \le \omega \le \pi$, as shown in (42) and (44). Since $P + S = N_i - 1$, we need one more sample which is placed at either ω_p or ω_s.

D. Band-Pass Filter Design

Without loss of generality, suppose that the band-pass filter to be designed is of Type I. Then its frequency response can be expressed as shown in (10). Let the filter have a passband

$\omega_{p_1} \leq \omega \leq \omega_{p_2}$, and two stopbands $0 \leq \omega \leq \omega_{s_1}$ and $\omega_{s_2} \leq \omega \leq \pi$, with peak ripples δ_p, δ_{s_1}, and δ_{s_2}, respectively.

As in low-pass filter design, the desired frequency response is represented by analytic functions, one for each band. The real-valued amplitude response $A(\omega)$ is represented by

$$A(\omega) = \begin{cases} H_{s_1}(\omega) = \delta_{s_1} T_{S_1}[X_{s_1}(\omega)], & 0 \leq \omega \leq \omega_{s_1} \\ H_p(\omega) = 1 - \delta_p T_P[X_p(\omega)], & \omega_{p_1} \leq \omega \leq \omega_{p_2} \\ H_{s_2}(\omega) = \delta_{s_2} T_{S_2}[X_{s_2}(\omega)] & \omega_{s_2} \leq \omega \leq \pi. \end{cases} \tag{62}$$

Here, P, S_1, and S_2 are the orders of the Chebyshev polynomials in the passband, first stopband, and second stopband, respectively. They are given by

$$P = \frac{N_p + 1}{2} \tag{63}$$

$$S_1 = N_{s_1} \tag{64}$$

$$S_2 = N_{s_2} \tag{65}$$

where N_p, N_{s_1}, and N_{s_2} represent the number of extrema in the frequency bands $\omega_{p_1} \leq \omega \leq \omega_{p_2}$, $0 \leq \omega \leq \omega_{s_1}$, and $\omega_{s_2} \leq \omega \leq \pi$, respectively. The functions, $X_p(\omega)$, $X_{s_1}(\omega)$ and $X_{s_2}(\omega)$, are required to map the equiripple intervals of the Chebyshev polynomials to the respective frequency bands. They are chosen to be of the form

$$X_p(\omega) = A \cos(a\omega + b) + B \tag{66}$$

$$X_{s_1}(\omega) = C \cos(c\omega + d) + D \tag{67}$$

$$X_{s_2}(\omega) = E \cos(e\omega + f) + F. \tag{68}$$

The twelve parameters involved are obtained by imposing appropriate constraints [9], [12] on the three functions, $H_p(\omega)$, $H_{s_1}(\omega)$, and $H_{s_2}(\omega)$. The results are included in Appendix A.

As shown in Section III-B, N_p, N_{s_1}, and N_{s_2} are found by weighting them in proportion to the sizes of the three respective frequency bands. The optimum filter response has a minimum of $(L + 2)$ alternations, where $L = (N - 1)/2$. This includes the alternations at the four bandedges ω_{s_1}, ω_{p_1}, ω_{p_2}, ω_{s_2}. Since the sum $N_p + N_{s_1} + N_{s_2}$ equals the total number of extrema in the range $0 \leq \omega \leq \pi$, it should be at least $(L - 2) = (N - 5)/2$. As with low-pass filter design, samples are placed at the extrema and bandedges in the range $0 \leq \omega \leq \pi$, so as to obtain $N_i = (N + 1)/2$ linear equations. Note that the sample locations are given by closed-form expressions similar to those found in Section III-B.

E. Third-Band Filter Design

Mth-band [13] filters are used for decimation and interpolation by a factor of M. Half-band filter design ($M = 2$) was discussed toward the end of Section III-B. The impulse response $h[n]$ of an Mth-band filter has one out of M samples equal to zero. These filters are restricted to be of Type I. Let the filter have length N, passband edge ω_p, stopband edge ω_s, and peak ripples δ_p and δ_s in the passband and stopband, respectively. The main properties of an Mth-band filter are as follows:

$$h[n] = \begin{cases} 0, & n - \dfrac{N-1}{2} = \text{nonzero multiple of } M \\ \dfrac{1}{M}, & n = \dfrac{N-1}{2} \end{cases} \tag{69}$$

$$\omega_p + \omega_s = \frac{2\pi}{M} \tag{70}$$

$$\delta_p \leq (M - 1)\delta_s. \tag{71}$$

The frequency response has a passband $0 \leq \omega \leq \omega_p$ and $(M - 1)$ stopbands interleaved with "don't-care" bands. The stopbands are defined by

$$\left[-\omega_p + \frac{2k\pi}{M}, \omega_p + \frac{2k\pi}{M}\right], \quad k = 1, 2, \cdots, M - 1.$$

As shown in [13], (69) requires that

$$\sum_{k=0}^{M-1} H\left(\omega + \frac{2\pi k}{M}\right) = Mh\left[\frac{N-1}{2}\right]. \tag{72}$$

For a filter with a normalized passband

$$h\left[\frac{N-1}{2}\right] = \frac{1}{M}. \tag{73}$$

By taking advantage of the zero-valued coefficients, an Mth-band filter achieves a computational reduction of nearly $1/M$ when compared with a general FIR filter of the same length.

We can use the proposed nonuniform sampling method to design an Mth-band FIR filter by mapping separate Chebyshev polynomials to the passband and $(M - 1)$ stopbands of the desired frequency response. Our technique can also utilize the knowledge of the zero-valued filter coefficients to obtain a reduced design time, as compared with general FIR filter design. From the condition in (69), the number of independent filter coefficients in an Mth-band filter is given by

$$N_i = \frac{N-1}{2} - \left\lfloor \frac{N-1}{2M} \right\rfloor. \tag{74}$$

Thus, we require N_i samples to design the filter. These samples are placed at the extrema and bandedges of the passband and stopbands. No samples are placed in the don't-care bands, since we do not have any particular desired response for these bands.

For clarity, we now consider the case of third-band filter design, where $M = 3$. The frequency response has a passband $0 \leq \omega \leq \omega_p$, a stopband $(2\pi/3 - \omega_p) \leq \omega \leq (2\pi/3 + \omega_p)$ and a don't-care band $(2\pi/3 + \omega_p) \leq \omega \leq \pi$. Thus, the stopband starts at the frequency $\omega_s = (2\pi/3 - \omega_p)$.

Since this is a Type I filter, its frequency response can be expressed as shown in (10). We express the real-valued amplitude response $A(\omega)$ in the form

$$A(\omega) = \begin{cases} H_p(\omega) = 1 - \delta_p T_P[X_p(\omega)], & 0 \leq \omega \leq \omega_p \\ H_s(\omega) = \delta_s T_S[X_s(\omega)], & \omega_s \leq \omega \leq \dfrac{2\pi}{3} + \omega_p. \end{cases} \tag{75}$$

The integers P and S are the orders of the Chebyshev polynomials in the passband and stopband, respectively. Since the widths of the passband and stopband are equal

$$P = S. \tag{76}$$

By recognizing that there are M bands in the frequency response, and that P equals the number of extrema in the region $0 \leq \omega \leq \omega_p$, we obtain

$$P = \left\lfloor \frac{N-1}{2M} \right\rfloor \tag{77}$$

where $M = 3$ for the third-band case. The functions $X_p(\omega)$ and $X_s(\omega)$ are chosen as in (17) and (18). The eight parameters involved are obtained by imposing constraints on the functions, $H_p(\omega)$ and $H_s(\omega)$, as shown in Section III-B. The only modifications for third-band filters arise because the stopband function $H_s(\omega)$ is assumed to symmetric about the point $\omega = 2\pi/3$. Thus, we have the new constraints

$$H_s\left(\frac{2\pi}{3} + \omega\right) = H_s\left(\frac{2\pi}{3} - \omega\right), \tag{78}$$

$$H_s\left(\frac{2\pi}{3}\right) = \begin{cases} -\delta_s, & S = \text{odd}, \\ \delta_s, & S = \text{even} \end{cases} \tag{79}$$

instead of those in (20) and (24). As derived in [9], we get new expressions for the following parameters:

$$c = -\frac{1}{\omega_p} \cos^{-1}\left(\frac{D-1}{C}\right) \tag{80}$$

$$d = \pi\left(1 - \frac{2c}{3}\right). \tag{81}$$

While choosing the sample locations, we must carefully consider the relation in (72) to pick the independent region of the frequency response. For the third-band case, we place samples at the extrema in the regions $0 \leq \omega \leq \omega_p$ and $\omega_s \leq \omega < 2\pi/3$, since the frequency response in the rest of the stopband is fully determined by the response in these regions. We compute the sample locations using closed-form expressions for the extrema, as discussed in Section III-B.

F. Design Examples

Example 1: The NDFT-based method is compared with other frequency sampling methods by considering the design of a Type I low-pass filter with specifications: $N = 37$, $\omega_p = 0.3\pi$, $\omega_s = 0.4\pi$, $\delta_p/\delta_s = 1$. The three uniform frequency sampling methods mentioned at the beginning of Section III are used: 1) original uniform frequency sampling with sample values of unity in the passband and zeros in the stopband, 2) uniform frequency sampling using linear programming to optimize the values of the samples in the transition band [3], and 3) modified uniform frequency sampling using analytic functions to approximate the desired frequency response [12]. For method 2, there is only one transition sample with the given specifications—its value is chosen to be 0.39, so as to minimize the peak stopband ripple. In method 3, the analytic functions generated in the first step of the NDFT–based method are sampled uniformly. Since some of these samples are located in the transition band, an additional function is required to approximate the frequency response in this band.

TABLE I
PERFORMANCE COMPARISON FOR FREQUENCY SAMPLING DESIGNS OF TYPE I LOW-PASS FILTER

Method	ω_p (π)	ω_s (π)	A_p (dB)	A_s (dB)	δ_p/δ_s
(1)	0.2790	0.3374	1.1512	16.0977	0.7921
(2)	0.2782	0.3740	0.4671	42.6863	7.1332
(3)	0.3103	0.3963	0.2404	33.6428	1.3130
NDFT	0.3006	0.4039	0.1121	37.7473	0.9894

This function is chosen to be a weighted linear combination of the passband and stopband functions as described in [12]. Table I provides a comparison of the bandedges, attenuation and ratio of peak ripples actually attained by these filters. A_p is the passband attenuation, defined as

$$A_p = -20 \log_{10}(1 - \delta_p) \tag{82}$$

where δ_p is the maximum ripple in the passband. A_s is the stopband attenuation, defined as

$$A_s = -20 \log_{10} \delta_s \tag{83}$$

where δ_s is the maximum ripple in the stopband. The passband and stopband edges of the filters designed are measured as

$$\omega_p = \max\{\omega | H(\omega) = 1 - \delta_p \quad \text{and} \quad 0 < \omega < \pi\} \tag{84}$$

and

$$\omega_s = \min\{\omega | \, |H(\omega)| = \delta_s \quad \text{and} \quad 0 < \omega < \pi\}. \tag{85}$$

Table I clearly shows that the NDFT method provides the closest overall match to the desired specifications. For example, although method 2 provides the highest A_s, this is obtained at the expense of a δ_p/δ_s which far exceeds the desired value of unity ($\delta_p/\delta_s = 7.1332$). Since methods 1 and 2 provide inadequate control over the bandedges and no control over the ratio of the passband and stopband ripples, we do not use them in the remaining examples.

Example 2: To further demonstrate the performance of the proposed nonuniform frequency sampling method, we design filters with the following sets of specifications: 1) half-band low-pass filter: $N = 55$, $\omega_p = 0.46\pi$, $\omega_s = 0.54\pi$; 2) low-pass filter of Type II: $N = 46$, $\omega_p = 0.35\pi$, $\omega_s = 0.45\pi$, $\delta_p/\delta_s = 3$, 3) third-band filter: $N = 23$, $\omega_p = 0.2\pi$, stopband from $\omega_{s_1} = 0.4667\pi$ to $\omega_{s_2} = 0.8667\pi$. For each set, three filter design methods are used—the NDFT method, Parks–McClellan algorithm [11] and modified uniform frequency sampling (referred to as the DFT method here) [12]. Note that the DFT method cannot be used for third-band filter design, due to the presence of the don't-care band. We compare the performances of these methods in Tables II and III. The design times required are shown in the last column of each table. As expected, the times are the largest when the iterative Parks–McClellan algorithm is used. Much smaller times are required by the

TABLE II
PERFORMANCE COMPARISON FOR HALF-BAND AND TYPE II LOW-PASS FILTER DESIGN

Filter	Method	ω_p (π)	ω_s (π)	A_p (dB)	A_s (dB)	Time (sec)
Half-band lowpass	NDFT	0.4593	0.5407	0.0544	44.0894	0.0833
	PM	0.4600	0.5400	0.0572	43.6580	11.4833
	DFT	0.4619	0.5381	0.1052	38.3880	0.1000
Type II lowpass	NDFT	0.3501	0.4531	0.0799	49.0769	0.1833
	PM	0.3500	0.4501	0.0906	49.2479	6.3667
	DFT	0.3512	0.4467	0.1288	45.0239	0.1167

TABLE III
PERFORMANCE COMPARISON FOR THIRD-BAND FILTER DESIGN

Method	ω_p (π)	ω_{s_1} (π)	ω_{s_2} (π)	A_p (dB)	A_s (dB)	Time (sec)
NDFT	0.2014	0.4662	0.8709	0.0139	60.8634	0.1333
PM	0.2000	0.4663	0.8673	0.0139	60.9417	3.1500

frequency sampling methods, both uniform and nonuniform. The filters designed by the nonuniform frequency sampling method come much closer to optimal filters. Note that the stopband attenuations (A_s) of the filters designed by the NDFT and Parks–McClellan methods differ by only about 1 dB.

Example 3: In this example, we illustrate the details of the proposed method by considering the design of a Type I band-pass filter, as discussed in Section III-D. The given filter specifications are: $N = 51$, $\omega_{s_1} = 0.2\pi$, $\omega_{p_1} = 0.25\pi$, $\omega_{p_2} = 0.6\pi$, $\omega_{s_2} = 0.65\pi$, $\delta_p = \delta_{s_1} = \delta_{s_2}$. The orders of the three Chebyshev polynomials are: $P = 6$, $S_1 = 6$, $S_2 = 8$. Fig. 1(a) shows the three functions $H_p(\omega)$, $H_{s_1}(\omega)$, and $H_{s_2}(\omega)$, approximating the passband and two stopbands of the desired band-pass response. These functions are sampled at the locations denoted by "$*$" in this figure. The resulting filter has a frequency response that is nearly equiripple, as shown in Fig. 1(b).

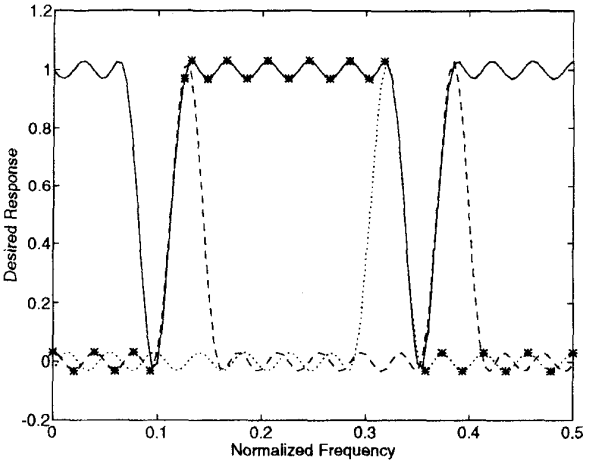

(a)

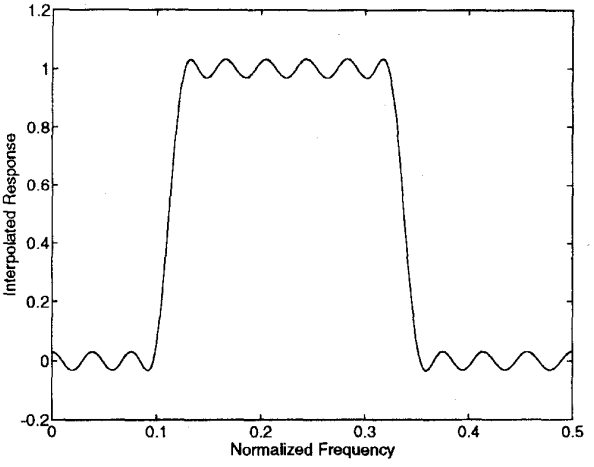

(b)

Fig. 1. Band-pass filter design example. (a) Functions $H_p(\omega)$ (solid line), $H_{s_1}(\omega)$ (dashed line), and $H_{s_2}(\omega)$ (dotted line) approximate the three bands of the desired response. The samples are denoted by "$*$." (b) Interpolated response of resulting band-pass filter.

G. Results

In many cases, the filters designed by the proposed nonuniform frequency sampling method are *very close to optimal* equiripple filters. This was illustrated by the preceding design examples. The design time required by the NDFT method is *much lower*, when compared to iterative optimization methods such as the Parks–McClellan algorithm. Although extensive testing is required for a thorough performance comparison between these methods, we have obtained some preliminary results by recording the times taken by both methods to design low-pass filters with fixed bandedges and increasing lengths. Fig. 2 shows the variation of design time with filter length for the NDFT method and Parks–McClellan algorithm. The simulations were performed on a Sun SPARC-2 workstation. From the comparison presented in Fig. 2, it is clear that the NDFT method is particularly useful for designing long filters, since iterative routines need excessively large amounts of time in such cases. The proposed method can be used to design a nearly optimal filter in a much shorter time.

All symmetries in the filter impulse response are utilized in the proposed method, so that we need to solve for only the independent filter coefficients. For example, the presence of alternating zeros in the impulse response of half-band filters has been utilized, reducing the design time by a factor of half. In third-band filter design, we chose not to place any samples in the don't-care frequency band. These illustrate the flexibility of nonuniform frequency sampling.

We have proposed a choice of extremal frequencies based on a nonuniform sampling of analytic functions derived from Chebyshev polynomials. This set of extrema can also be used as a good starting point for the Parks–McClellan algorithm, if exactly optimal filters are to be designed. We have performed simulations to compare the performances of this algorithm with two different starting points: 1) the proposed nonuniform

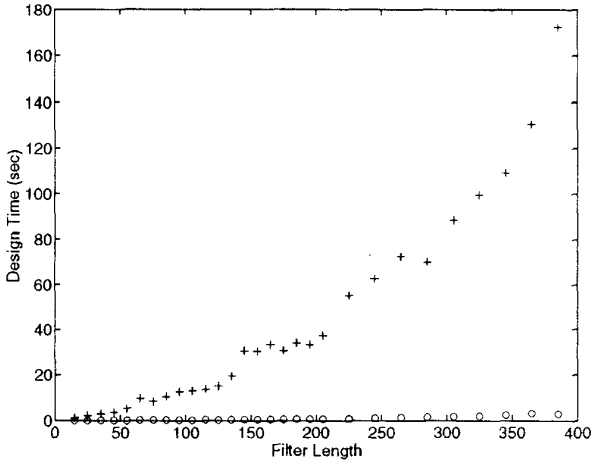

Fig. 2. Plot of filter design time with filter length, for the NDFT method ("o") and Parks–McClellan algorithm ("+").

choice of extrema, and 2) the standard uniform choice of extrema. Our results show that the nonuniform choice of extrema *decreases* the number of iterations required, as well as the design time. Fig. 3 shows the variation of each of these quantities with filter length using the two starting points. These plots were obtained by designing a low-pass filter with fixed bandedges, and gradually increasing the filter length.

H. Choice of Extrema as Sample Locations

The results shown in Sections III-F and III-G demonstrate that the filters designed by the nonuniform frequency sampling method are very close to optimal minimax filters. We now consider the reasons behind our choice of extrema as sample locations. Note that the Parks–McClellan algorithm is based on the fact that an optimal minimax filter must have alternations at the extremal frequencies [10]. It starts with an initial guess for the extrema, fits a polynomial, checks the resulting ripple δ, and then searches for the new extremal frequencies. This cycle is repeated until δ does not change from its previous value by more than a specified small amount. Thus the initial guess of extrema is improved in successive iterations until the optimal filter is obtained.

In our method, we generate a good approximation to the desired frequency response, and then sample this at the extrema to obtain the linear equations required to solve for the impulse response coefficients. We now show that this choice of sample locations *minimizes* the sensitivity of the frequency response to a perturbation in the sample locations. Let $D(z)$ be the desired response, and $H(z)$ be the actual filter response obtained, i.e., the resulting filter polynomial of order $N-1$. We solve for the N coefficients of $H(z)$ by taking N samples

$$H(z_k) = D(z_k), \quad k = 0, 1, \cdots, N-1. \tag{86}$$

The function $H(z)$ can be written explicitly as a function of not only the variable z, but also the sample locations $z_0, z_1, \cdots, z_{N-1}$, since the impulse response coefficients

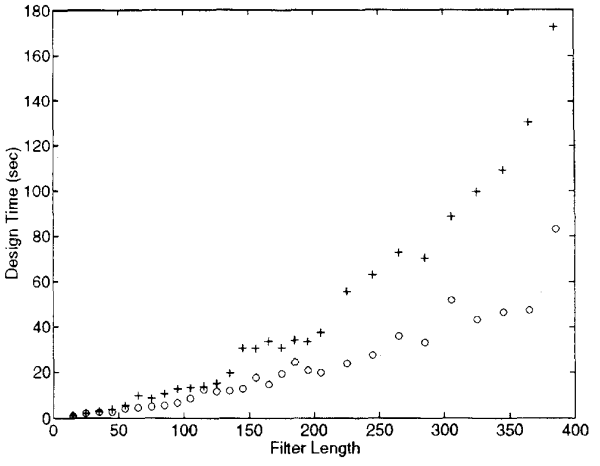

(a)

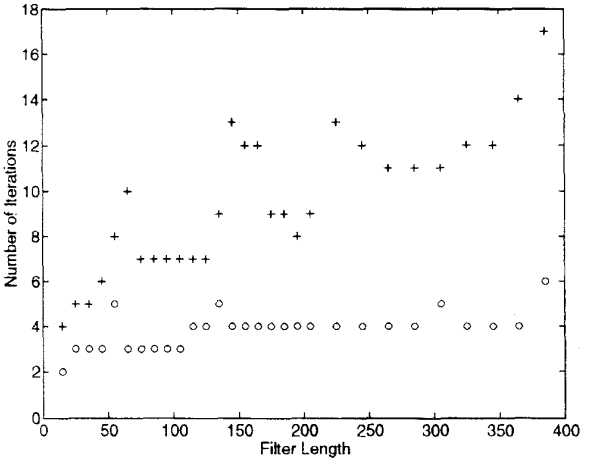

(b)

Fig. 3. Comparison of different starting points for the Parks–McClellan algorithm, denoted by "o" for proposed nonuniformly spaced extrema, and "+" for standard uniformly spaced extrema. (a) Plot of design time with filter length. (b) Plot of number of iterations with filter length.

depend on them. This gives the following form

$$H(z) = F(z_0, z_1, \cdots, z_{N-1}, z). \tag{87}$$

Therefore the samples can be expressed as

$$H(z_k) = F(z_0, z_1, \cdots, z_{N-1}, z_k). \tag{88}$$

To study the effect of varying the frequency-sample location z_k on the frequency response $H(z)$, we differentiate both sides of (86) with respect to z_k to get

$$\frac{\partial H(z_k)}{\partial z_k} = \frac{\partial D(z_k)}{\partial z_k} = \frac{\partial D(z)}{\partial z}\bigg|_{z=z_k}. \tag{89}$$

Differentiating both sides of (88) with respect to z_k, we get

$$\frac{\partial H(z_k)}{\partial z_k} = \left.\frac{\partial H(z)}{\partial z_k}\right|_{z=z_k} + \left.\frac{\partial H(z)}{\partial z}\right|_{z=z_k}. \tag{90}$$

Comparing (89) and (90), we obtain

$$\left.\frac{\partial D(z)}{\partial z}\right|_{z=z_k} = \left.\frac{\partial H(z)}{\partial z_k}\right|_{z=z_k} + \left.\frac{\partial H(z)}{\partial z}\right|_{z=z_k} \tag{91}$$

or

$$\begin{aligned}\left.\frac{\partial H(z)}{\partial z_k}\right|_{z=z_k} &= \left.\frac{\partial D(z)}{\partial z}\right|_{z=z_k} - \left.\frac{\partial H(z)}{\partial z}\right|_{z=z_k} \\ &= \left.\frac{\partial E(z)}{\partial z}\right|_{z=z_k}\end{aligned} \tag{92}$$

where $E(z)$ is the interpolation error function defined as

$$E(z) = D(z) - H(z). \tag{93}$$

The quantity on the left hand side of (92) is the sensitivity of the frequency response at the point z_k to a small perturbation in the location of the kth sample. This sensitivity equals the difference in slopes of $D(z)$ and $H(z)$ at $z = z_k$, i.e., the slope of the interpolation error at this point. If we sample at the extrema of $D(z)$, the slope of $D(z)$ is zero at these points. Since these points lie close to the extrema of $H(z)$ actually obtained, the slope of $H(z)$ is also nearly zero there. Thus the resulting sensitivities at these points are close to zero. Therefore the extrema are good locations for the samples from this point of view.

Finally, we present a numerical example to demonstrate that if we perturb the location of a sample away from the extremum, the peak ripple in that particular frequency band increases.

Example 4: Consider the design of a low-pass filter with the following specifications: $N = 37$, $\omega_p = 0.4\pi$, $\omega_s = 0.5\pi$, $\delta_p/\delta_s = 1$. By using our design method, we obtain a nearly equiripple filter with the following values for the peak attenuation in the passband and stopband, respectively: $A_p = 0.0956$ dB, $A_s = 36.9301$ dB.

Now, we vary the location of one sample in the passband on either side of the extremum, and redesign the filter for each new sample location. Fig. 4(a) shows the variation of A_p with change in sample frequency about the extremum. This plot shows that the lowest passband attenuation is obtained when the sample is at the extremum. This process is repeated by varying the location of one sample in the stopband about the extremum. Fig. 4(b) shows that the resulting stopband attenuation is maximum when the sample is at the extremal frequency.

Next, we simultaneously vary the locations of two adjacent samples in the passband about their respective extremal positions. The filter is redesigned for each new pair of locations. Fig. 5(a) shows the values of A_p obtained in these situations.

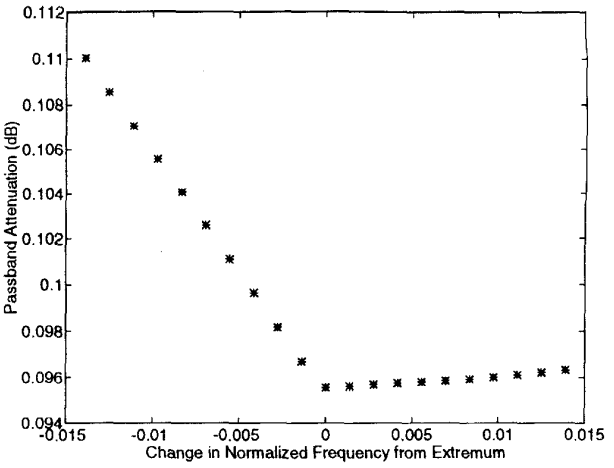

(a)

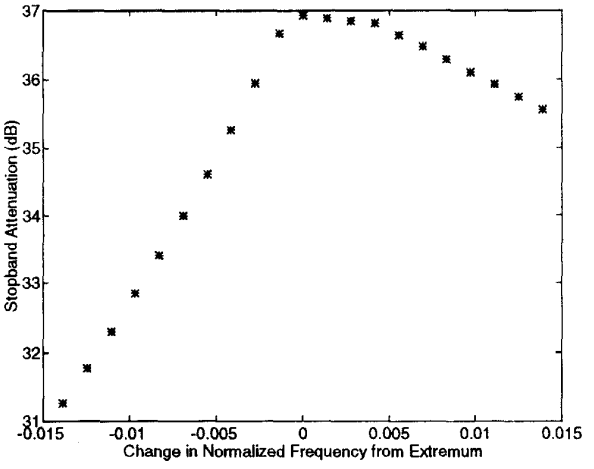

(b)

Fig. 4. Effects of varying the location of one sample away from the extremum. (a) Passband attenuation A_p, with change in frequency of a sample in the passband. (b) Stopband attenuation A_s, with change in frequency of a sample in the stopband.

Again, the passband attenuation is minimum when both samples are at the extrema. This procedure is repeated by varying, simultaneously, the locations of two adjacent samples in the stopband. Fig. 5(b) shows the resulting stopband attenuation, which reaches a maximum when both samples are at the extrema.

This example demonstrates that the extrema form a good choice of sample locations for filter design, from the point of view of minimizing the peak ripples.

IV. Conclusion

The concept of the nonuniform discrete Fourier transform, which corresponds to a nonuniform sampling of the z-transform, was proposed in this paper. The main advantage of the NDFT is the flexibility which it provides in locating samples in the z-domain. The conventional DFT is a special case of the NDFT, obtained when the sampling points are located on the unit circle at equally spaced angles. We

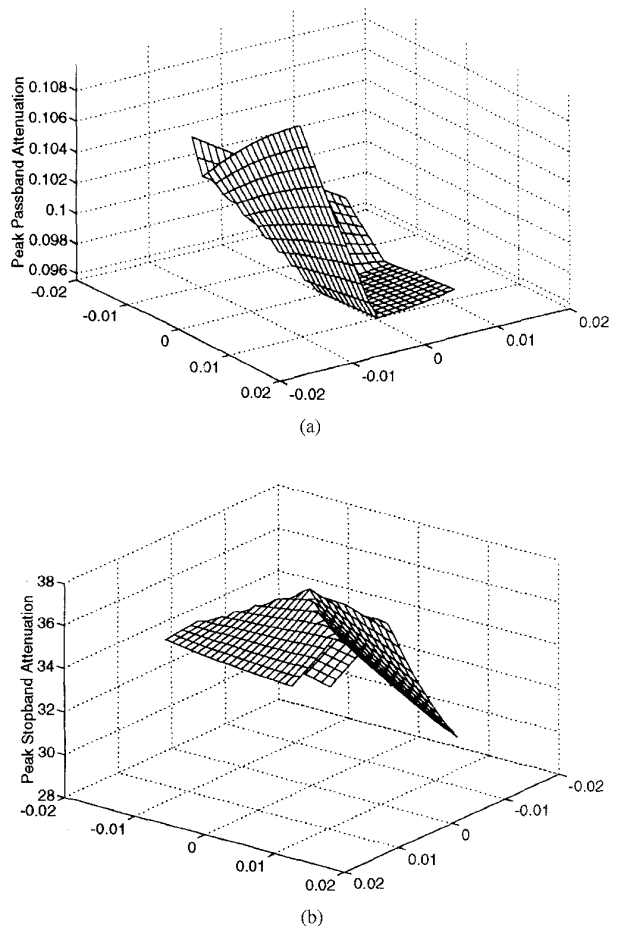

Fig. 5. Effects of varying the locations of two adjacent samples away from the extrema. (a) Passband attenuation A_p, with change in frequencies of two samples in the passband. (b) Stopband attenuation A_s, with change in frequencies of two samples in the stopband.

utilized the NDFT to develop a new nonuniform frequency sampling method for designing 1-D FIR filters. Although there have been some earlier efforts to design 1-D filters using nonuniform frequency samples, no working design technique existed before. The proposed method produces nearly optimal equiripple filters, as demonstrated by the design examples presented in Section III-F. Since the design times required are much smaller than for exactly optimal filters, this method is particularly useful for designing long filters. Moreover, the proposed choice of nonuniform extremal frequencies can be used as a good starting point for the Parks–McClellan algorithms, if truly optimal filters are desired. The results obtained also illustrate the advantages of nonuniform frequency sampling over uniform sampling. The NDFT has also been used in other applications such as antenna pattern synthesis with prescribed nulls, and dual-tone multifrequency (DTMF) tone detection [9]. The results obtained illustrate the potential of the NDFT in successfully solving problems that involve nonuniform sampling in the frequency domain. In a companion paper [7], we show how the flexibility available in locating the frequency samples becomes even more important, when applied to the 2-D case.

APPENDIX A

For type I band-pass filter design, let ω_m be the center of the passband. Then $H_p(\omega)$ is assumed to be symmetric about $\omega = \omega_m$. Further, let $\delta_s = \max(\delta_{s_1}, \delta_{s_2})$. Then, we restrict the functions, $X_p(\omega)$, $X_{s_1}(\omega)$, and $X_{s_2}(\omega)$, to stay between $-\delta_s$ and $(1+\delta_p)$ at all frequencies. Thus, the constraints used are

$$\begin{aligned}
H_p(\omega_m + \omega) &= H_p(\omega_m - \omega) \\
H_{s_1}(\omega) &= H_{s_1}(-\omega) \\
H_{s_2}(\pi + \omega) &= H_{s_2}(\pi - \omega) \\
H_p(\omega_{p_1}) &= 1 - \delta_p \\
H_{s_1}(\omega_{s_1}) &= \delta_{s_1} \\
H_{s_2}(\omega_{s_2}) &= \delta_{s_2} \\
H_p(\omega_m) &= \begin{cases} 1+\delta_p, & P = \text{odd} \\ 1-\delta_p, & P = \text{even} \end{cases} \\
H_{s_1}(0) &= \begin{cases} -\delta_{s_1}, & S_1 = \text{odd} \\ \delta_{s_1}, & S_1 = \text{even} \end{cases} \\
H_{s_2}(\pi) &= \begin{cases} -\delta_{s_2}, & S_2 = \text{odd} \\ \delta_{s_2}, & S_2 = \text{even} \end{cases} \\
\min[H_p(\omega)] &= -\delta_s \\
\max[H_{s_1}(\omega)] &= 1 + \delta_p \\
\max[H_{s_2}(\omega)] &= 1 + \delta_p.
\end{aligned}$$

These lead to the following expressions for the parameters

$$\begin{aligned}
A &= \frac{1}{2}\left\{T_P^{-1}\left(\frac{1+\delta_s}{\delta_p}\right)+1\right\} \\
B &= A - 1 \\
C &= \frac{1}{2}\left\{T_{S_1}^{-1}\left(\frac{1+\delta_p}{\delta_{s_1}}\right)+1\right\} \\
D &= C - 1 \\
E &= \frac{1}{2}\left\{T_{S_2}^{-1}\left(\frac{1+\delta_p}{\delta_{s_2}}\right)+1\right\} \\
F &= E - 1 \\
a &= \frac{1}{\omega_{p_1} - \omega_m}\cos^{-1}\left(\frac{B-1}{A}\right) \\
b &= \pi - a\omega_m \\
c &= \frac{1}{\omega_{s_1}}\cos^{-1}\left(\frac{D-1}{C}\right) \\
d &= \pi \\
e &= \frac{1}{\omega_{s_2} - \pi}\cos^{-1}\left(\frac{F-1}{E}\right) \\
f &= \pi(1-e).
\end{aligned}$$

REFERENCES

[1] L. R. Rabiner, R. W. Schafer, and C. M. Rader, "The chirp z-transform algorithm," *IEEE Trans. Audio Electroacoust.*, vol. AU-17, pp. 86–92, June 1969.

[2] A. Oppenheim and D. Johnson, "Computation of spectra with unequal resolution using the fast Fourier transform," *Proc. IEEE*, vol. 59, pp. 299–301, Feb. 1971.

[3] L. R. Rabiner, B. Gold, and C. A. McGonegal, "An approach to the approximation problem for nonrecursive digital filters," *IEEE Trans. Audio Electroacoust.*, vol. AU-18, pp. 83–106, June 1970.

[4] E. Angelides and J. E. Diamessis, "A novel method for designing FIR digital filters with nonuniform frequency samples," *IEEE Trans. Acoust., Speech, Signal Processing*, vol. 42, pp. 259–267, Feb. 1994.

[5] E. Angelides, "A recursive frequency-sampling method for designing zero-phase FIR filters by nonuniform samples," *IEEE Trans. Signal Processing,* vol. 6, pp. 1461–1467, June 1995.
[6] S. K. Mitra, S. Chakrabarti, and E. Abreu, "Nonuniform discrete Fourier transform and its applications in signal processing," in *Proc. EUSIPCO '92, Sixth Euro. Signal Processing Conf.,* Brussels, Belgium, Aug. 1992, vol. 2, pp. 909–912.
[7] S. Bagchi and S. K. Mitra, "The nonuniform discrete Fourier transform and its applications in filter design: II—2-D," this issue, pp. 434-444.
[8] P. J. Davis, *Interpolation and Approximation.* New York: Dover, 1975.
[9] S. Bagchi, "The nonuniform discrete Fourier transform and its applications in signal processing," Ph.D. dissertation, Univ. California, Santa Barbara, 1994.
[10] A. V. Oppenheim and R. W. Schafer, *Discrete-Time Signal Processing.* Englewood Cliffs, NJ: Prentice-Hall, 1989.
[11] J. H. McClellan, T. W. Parks, and L. R. Rabiner, "A computer program for designing optimum FIR linear phase digital filters," *IEEE Trans. Audio Electroacoust.,* vol. AU-21, pp. 506–526, Dec. 1973.
[12] M. Lightstone, S. K. Mitra, I.-S. Lin, S. Bagchi, P. Jarske, and Y. Neuvo, "Efficient frequency-sampling design of one-and two-dimensional FIR filters using structural subband decomposition," *IEEE Trans. Circuits Syst. II,* vol. 41, pp. 189–201, Mar. 1994.
[13] F. Mintzer, "On half-band, third-band and Nth band FIR filters and their design," *IEEE Trans. Acoust., Speech, Signal Processing,* vol. ASSP-30, pp. 734–738, Oct. 1982.

Sonali Bagchi (S'90–M'95) received the B.Tech. (honors) degree in electronics and electrical communication engineering from the Indian Institute of Technology, Kharagpur, India, in 1989; the M.S. degree in electrical engineering from the California Institute of Technology, Pasadena, in 1990; and the Ph.D. degree in electrical and computer engineering from the University of California at Santa Barbara in 1994.

In 1993, she worked as a summer intern in the Communication Systems Research Laboratory of Tektronix, Inc., in the areas of 2-D digital filtering and image compression. Since 1994, she has been with the Modem and Multimedia Group of AT&T Bell Laboratories as a Member of Technical Staff. Her current research interests include digital signal processing, communications, and VLSI design.

Sanjit K. Mitra (SM'69–F'74) received the B.Sc. (Hons.) degree in physics in 1953 from Utkal University, Cuttack, India; the M.Sc. (Tech.) degree in radio physics and electronics in 1956 from Calcutta University, India; and the M.S. and Ph.D. degrees in electrical engineering from the University of California, Berkeley, in 1960 and 1962, respectively.

From June 1962 to June 1965, he was with Cornell University, Ithaca, NY, as an Assistant Professor of electrical engineering. He was with AT&T Bell Laboratories, Holmdel, NJ, from June 1965 to January 1967. He has been on the faculty of the University of California since then, first at the Davis campus and more recently at the Santa Barbara campus, as a Professor of electrical and computer engineering, where he served as Chairman of the Department from July 1979 to June 1982.

Dr. Mitra is the recipient of the 1973 F.E. Terman Award and the 1985 AT&T Foundation Award of the American Society of Engineering Education, the Education Award of the IEEE Circuits and Systems Society in 1989, the Distinguished Senior U.S. Scientist Award from the Alexander von Humboldt Foundation of West Germany in 1989, and the Technical Achievement Award of the IEEE Signal Processing Society in 1996. In May 1987 he was awarded an Honorary Doctorate of Technology degree from the Tampere University of Technology, Tampere, Finland. He served as the President of the IEEE Circuits and Systems Society in 1986. He is currently a member of the editorial boards of the *International Journal on Circuits, Systems and Signal Processing*, *International Journal on Multidimensional Systems and Signal Processing*; *Signal Processing*; and the *Journal of the Franklin Institute*. He is a Fellow of the AAAS and SPIE, and a member of EURASIP and ASEE.